PERFORMANCE CHARACTERISTICS OF COLLABORATIVE BEAMFORMING FOR WIRELESS SENSOR NETWORKS WITH GAUSSIAN DISTRIBUTED SENSOR NODES

Mohammed F. A. Ahmed *Sergiy A. Vorobyov*

Dept. of Electrical and Computer Engineering, University of Alberta, Edmonton, AB, Canada.
Email: mfahmed, vorobyov@ece.ualberta.ca

ABSTRACT

Collaborative beamforming has been recently introduced in the context of wireless sensor networks (WSNs) to increase the transmission range of individual sensor nodes. In this paper, it is proposed to model the spatial distribution of sensor nodes in a cluster using Gaussian probability density function (pdf). Gaussian pdf is more appropriate for many WSN applications than the previously considered uniform pdf which is more suitable when sensor nodes are deployed one at a time. The average beampattern and its characteristics, the distribution function of the beampattern level in the sidelobe region, and the upper bound on the outage probability of sidelobes are derived using the theory of random arrays.

Index Terms— Random arrays, cooperative systems, Gaussian distributions, array signal processing, phased arrays.

1. INTRODUCTION

In WSN applications, it is required to transmit the acquired data over long distances using the transmission resources available at sensor nodes only. However, this can be power costly for individual sensor nodes. The transmission range of sensor nodes can be extended based on the collaborative beamforming principle [1], [2]. This principle uses the fact that WSN can be deployed in the form of disjointed clusters of sensor nodes, which act collaboratively as distributed antenna arrays. Each sensor node shares the data to be transmitted with all other nodes in the cluster, and the same data symbols are transmitted by all nodes synchronously. The individual signals from sensor nodes arrive in phase and constructively add at the intended destination which can be a neighboring cluster or a base station.

Some characteristics of the collaborative beamformer average beampattern have been derived in [1] using the theory of random arrays [3], [4]. However, it has been assumed in [1] that the sensor nodes in each cluster are located according to uniform pdf. Selecting a suitable spatial pdf is a critically important problem because the characteristics of a sample beampattern are determined by the actual spatial distribution of sensor nodes. The assumption of uniform pdf is not well justified in many WSN applications because the actual pdf depends on the sensor nodes deployment method and can not be arbitrarily selected. For example, in some applications it is required to cover large geographical area. In this case, the deployment has to be done by dropping clusters of sensor nodes from an airplane. Then the spatial distribution of sensor nodes within a cluster is likely to be Gaussian [5].

Supported in part by the Natural Science and Engineering Research Council (NSERC) of Canada and the Alberta Ingenuity Foundation, Alberta, Canada. S.A. Vorobyov is on leave from the Joint Research Institute, Heriot-Watt University and the University of Edinburgh, Edinburgh, UK.

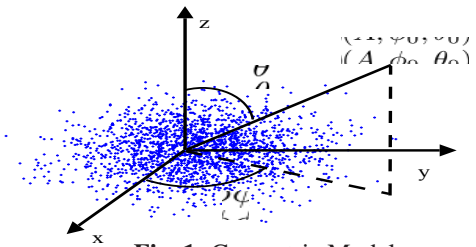

Fig. 1. Geometric Model.

In this paper, Gaussian pdf is used to model the spatial distribution of the sensor nodes in a cluster of WSN. The average beampattern characteristics are derived and compared with the corresponding characteristics for the case when uniform pdf is used. The distribution of the beampattern level in the sidelobe region as well as the upper bound on the outage probability of sidelobes are derived.

2. SYSTEM MODEL

Fig. 1 shows the geometric model of a cluster of N sensor nodes. For the spherical coordinates (r, ϕ, θ), the angle θ denotes the elevation direction, ϕ represents the azimuth direction, and r is the distance from the origin to a given point. Sensor nodes are co-located in the xy-plane. Therefore, for the kth sensor node we can write that $\theta_k = \frac{\pi}{2}$, $k = 1, \ldots, N$. The rectangular coordinates of the sensor nodes (x_k, y_k), $k = 1, \ldots, N$, are chosen randomly according to a zero mean Gaussian distribution with variance σ^2. The corresponding spherical coordinates $\left(r_k = \sqrt{x_k^2 + y_k^2},\ \phi_k = \tan^{-1}(\frac{y_k}{x_k})\right)$ have Rayleigh and uniform distributions, respectively, i.e., $f_{r_k}(r) = \frac{r}{\sigma^2} e^{-\frac{r^2}{2\sigma^2}};\ 0 \leq r < \infty$ and $f_{\phi_k}(\phi) = \frac{1}{2\pi};\ -\pi \leq \phi < \pi$.

Let us denote the Euclidean distance between the kth sensor node and a point (A, ϕ, θ) on a sphere of radius $r = A$ as $d_k(\phi, \theta) = \sqrt{A^2 + r_k^2 - 2r_k A \sin(\theta)\cos(\phi - \phi_k)}$. Assuming that the destination cluster or base station is located at (A, ϕ_0, θ_0), and defining the vectors $\mathbf{r} = [r_1, r_2, \ldots, r_N] \in [0, \infty]^N$ and $\boldsymbol{\phi} = [\phi_1, \phi_2, \ldots, \phi_N] \in [-\pi, \pi]^N$, the sample array factor for a cluster of randomly located sensor nodes can be defined as

$$F(\phi, \theta/\mathbf{r}, \boldsymbol{\phi}) \triangleq \frac{1}{N} \sum_{k=1}^{N} e^{j\psi_k} e^{j\frac{2\pi}{\lambda} d_k(\phi,\theta)} \tag{1}$$

where λ is the wavelength and ψ_k is initial phase of the kth sensor carrier frequency. The factor $1/N$ is used to insure that $\max[F(\phi, \theta/\mathbf{r}, \boldsymbol{\phi})]$=1. Assuming that the sensor nodes are aware of each other locations and synchronizing their carriers with initial phase $\psi_k = -\frac{2\pi}{\lambda} d(\phi_0, \theta_0)$, we can write the sample array factor as $F(\phi, \theta/\mathbf{r}, \boldsymbol{\phi}) = \frac{1}{N} \sum_{k=1}^{N} e^{j\frac{2\pi}{\lambda}[d_k(\phi,\theta) - d_k(\phi_0,\theta_0)]}$. Moreover, using the approximation $d_k(\phi, \theta) \approx A - r_k \sin(\theta)\cos(\phi - \phi_k)$, which is valid for the far-field region with $A \gg r_k$, we obtain that

$$F(\phi, \theta/\mathbf{r}, \boldsymbol{\phi}) \approx \frac{1}{N} \sum_{k=1}^{N} \exp\left\{ j\frac{2\pi}{\lambda} r_k [\sin(\theta_0)\cos(\phi_0 - \phi_k) - \sin(\theta)\cos(\phi - \phi_k)] \right\} \triangleq \tilde{F}(\phi, \theta/\mathbf{r}, \boldsymbol{\phi}). \tag{2}$$

Note that (2) is symmetric with respect to the azimuth direction ϕ. Therefore, we can set $\phi_0 = 0$. For notation simplicity, we also assume that the destination point is located in the xy-plane, i.e., $\theta = \theta_0 = \frac{\pi}{2}$. Then, (2) simplifies to $\tilde{F}(\phi/\mathbf{r}, \boldsymbol{\phi}) = \frac{1}{N} \sum_{k=1}^{N} e^{-j4\pi\tilde{r}_k \sin(\frac{\phi}{2}) \sin(\tilde{\phi}_k)}$, where $\tilde{r}_k = \frac{r_k}{\lambda}$ and $\tilde{\phi}_k = (\phi_k - \frac{\phi}{2})$. Equivalently, we can write that

$$\tilde{F}(\phi/\mathbf{z}) = \frac{1}{N} \sum_{k=1}^{N} e^{-j\alpha z_k} \tag{3}$$

where $\alpha = \alpha(\phi) = 4\pi \sin(\frac{\phi}{2})$, $\mathbf{z} = [z_1, z_2, \ldots, z_N] \in [-\infty, \infty]^N$, and the random variable $z_k = \tilde{r}_k \sin(\tilde{\phi}_k)$ is Gaussian distributed with zero mean and variance σ^2, i.e.,

$$f_{z_k}(z) = \frac{1}{\sqrt{2\pi}\sigma} e^{\frac{-z^2}{2\sigma^2}}, \quad -\infty < z < \infty. \tag{4}$$

Then, for each realization of $\mathbf{z}$, the sample far-field beampattern can be found as

$$P(\phi/\mathbf{z}) = |\tilde{F}(\phi/\mathbf{z})|^2 = \frac{1}{N} + \frac{1}{N^2} \sum_{k=1}^{N} e^{-j\alpha z_k} \sum_{\substack{l=1, \\ l \neq k}}^{N} e^{j\alpha z_l}. \tag{5}$$

3. AVERAGE BEAMPATTERN AND ITS CHARACTERISTICS

Using (4) and (5), the average beampattern for a cluster of Gaussian distributed sensor nodes can be obtained as

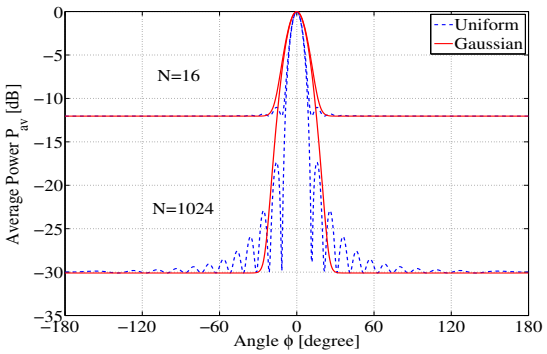

Fig. 2. Average beampatterns for both uniform and Gaussian spatial distributions: $N = 16$ and 1024, $\sigma^2 = 1$, $\tilde{R} = 3\sigma$.

$$P_{\text{av}}(\phi) = E_z[P(\phi/\mathbf{z})] = \frac{1}{N} + \left(1 - \frac{1}{N}\right) \left| e^{-\frac{\alpha^2\sigma^2}{2}} \right|^2 \tag{6}$$

where $E_z[\cdot]$ denotes the average over all realizations of z. The term $1/N$ in (6) represents the mean of the beampattern in the sidelobe region and it can be reduced by increasing N. It can also be seen from (6) that the average beampattern has no nulls and no sidelobes. Moreover, the mainlobe decays exponentially with a rate proportional to the variance σ^2. The average beampattern (6) is similar to the beampattern for uniformly distributed sensor nodes.[1] However, in the latter case, the Bessel function of the first kind results in nulls and sidelobes in the average beampattern. It is worth noting that the presence of sidelobes in the average beampattern increases the chance of sidelobes with high peaks in the sample beampatterns.

The average beampatterns for both cases of Gaussian and uniform spatial distributions are shown in Fig. 2, where $\sigma^2 = 1$, and $N \in \{16, 1024\}$. Hereafter, we use $\sigma = \frac{\tilde{R}}{3}$ in the case of Gaussian spatial distribution, where $\tilde{R}$ is defined for uniform distribution. This assumption suggests that 99.73% of the sensor nodes are located on a disk of radius $\tilde{R}$ and, thus, the cluster areas in both cases are the same. It can be seen from Fig. 2 that the mainlobe in the case of Gaussian spatial distribution is wider than in the case of uniform spatial distribution. In both cases, the width of the mainlobe can be reduced by increasing $\tilde{R} = 3\sigma$, i.e., by spreading the sensor nodes over a larger area.

The 3dB Beamwidth is defined as the angle $\phi_{3\text{dB}}$ at which the power of the average beampattern drops 3dB below the maximum value at $\phi = 0$. In the case of Gaussian distributed sensor nodes, the 3dB beamwidth can be expressed as [6]

$$\phi_{3\text{dB}} = 2\sin^{-1}\left(\frac{0.0663}{\sigma}\right). \tag{7}$$

[1] Note that the average beampattern in the case of uniformly distributed sensor nodes is given as [1]: $P_{\text{av}}(\phi) = \frac{1}{N} + (1 - \frac{1}{N}) \left| 2\frac{J_1(\alpha)}{\alpha} \right|^2$, where $J_1(\alpha)$ is the first order Bessel function of the first kind, $\alpha = \alpha(\phi) = 4\pi\tilde{R}\sin(\frac{\phi}{2})$, and the cluster is represented by a disk of radius $\tilde{R} = R/\lambda$.

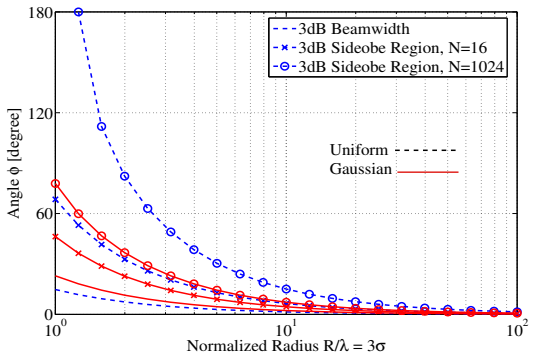

Fig. 3. 3dB beamwidth and 3dB sidelobe region for both uniform and Gaussian spatial distributions: $N = 16$ and 1024.

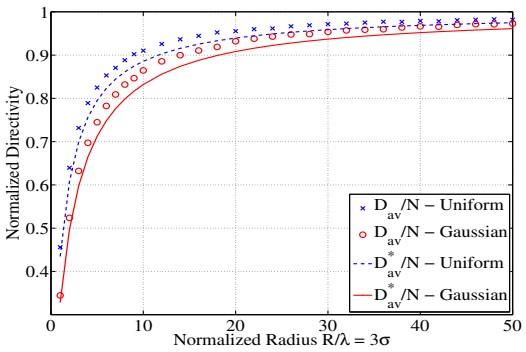

Fig. 4. $\frac{D_{\text{av}}}{N}$ and $\frac{D^*_{\text{av}}}{N}$ for both uniform and Gaussian spatial distributions: $N = 16$.

¿From (7), we can see that the 3dB beamwidth depends only on the variance σ^2 and it is independent of the number of sensor nodes.

The 3dB Sidelobe Region is the beampattern region between the angle ϕ_{Sidelobe} at which the mainlobe of the average beampattern reduces to 3dB above $1/N$ and π, i.e.,

$$\text{Sidelobe Region} = \{\phi \mid \phi_{\text{Sidelobe}} \leq |\phi| \leq \pi\}. \quad (8)$$

In the case of Gaussian spatial distribution, ϕ_{Sidelobe} is given by [6]

$$\phi_{\text{Sidelobe}} = 2\sin^{-1}\left(\frac{\sqrt{\ln(N-1)}}{4\pi\sigma}\right). \quad (9)$$

Fig. 3 shows the 3dB beamwidth and the 3dB sidelobe region for both uniform[2] and Gaussian spatial distributions versus the normalized radius $\tilde{R} = 3\sigma$. The beampattern in the case of Gaussian spatial distribution has larger 3dB beamwidth and sidelobe regions compared to the uniform case. The difference between the 3dB beamwidths for both distributions becomes smaller for larger normalized radius $\tilde{R} = 3\sigma$. Larger 3dB sidelobe region for the case of Gaussian spatial distribution suggests that the mean of the sample beampattern is close to the value $1/N$ over a larger area. Therefore, the sidelobes with high peaks are less probable in the case of Gaussian spatial distribution.

The Average Directivity, in the context of WSNs, represents the ability of the sensor nodes to concentrate the radiated power in a certain direction. The sample directivity given a realization of $\mathbf{z}$ can be expressed as

$$D(\mathbf{z}) = \frac{\int_{-\pi}^{\pi} P(0)d\phi}{\int_{-\pi}^{\pi} P(\phi/\mathbf{z})d\phi} = \frac{2\pi}{\int_{-\pi}^{\pi} P(\phi/\mathbf{z})d\phi} \quad (10)$$

where $P(0) = P(0/\mathbf{z}) = 1$. The average directivity can be defined as $D_{\text{av}} = E_z[D(\mathbf{z})]$, and its lower bound is given by $D^*_{\text{av}} = \frac{2\pi}{\int_{-\pi}^{\pi} P_{\text{av}}(\phi)d\phi}$ [1]. Using (6) and the expression for the lower bound on the average directivity, D^*_{av}, we can obtain

$$D^*_{\text{av}} = \frac{N}{1 + (N-1)\,{}_1F_1(\frac{1}{2}; 1; -(4\pi\sigma)^2)} \quad (11)$$

where ${}_1F_1(\frac{1}{2}; 1; -(4\pi\sigma)^2)$ is the hypergeometric function of the first kind.[3]

Fig. 4 shows the normalized average directivity $\frac{D_{\text{av}}}{N}$ and its normalized lower bound $\frac{D^*_{\text{av}}}{N}$ for both uniform and Gaussian spatial distributions. It can be seen from the figure that the directivity is lower in the case of Gaussian spatial distribution and approaches N asymptotically with increasing the normalized radius $\tilde{R} = 3\sigma$.

4. RANDOM BEHAVIOR OF SAMPLE BEAMPATTERN

Besides transmission range extension, the application of collaborative beamforming in the context of WSNs enables us to limit interference to neighboring clusters. Therefore, the complementary cumulative distribution function (CCDF) of the beampattern level in the sidelobe region should be small enough for any specific realization of the sensor node locations. The CCDF of the beampattern level at a given angle ϕ, for power level P_0, can be found as

$$\Pr[P(\phi) > P_0] = \int\int_{x^2+y^2>NP_0} f_{X,Y}(x,y)\,dx\,dy \quad (12)$$

where the array factor is approximated as a complex Gaussian random varaible, i.e., $\tilde{F}(\phi/\mathbf{z}) = \frac{1}{\sqrt{N}}(X - jY)$, and

$$f_{X,Y}(x,y) = \frac{1}{2\pi\sigma_x\sigma_y}\exp\left(-\frac{|x-m_x|^2}{2\sigma_x^2} - \frac{y^2}{2\sigma_y^2}\right). \quad (13)$$

In the case of Gaussian pdf, $m_x = \sqrt{N}e^{-\frac{\alpha^2\sigma^2}{2}}$, $\sigma_x^2 = \frac{1}{2}(1 + e^{-\frac{(2\alpha)^2\sigma^2}{2}}) - (e^{-\frac{\alpha^2\sigma^2}{2}})^2$, $m_y = 0$, and $\sigma_y^2 = \frac{1}{2}(1 - e^{-\frac{(2\alpha)^2\sigma^2}{2}})$.[4]

[2]Note that ϕ_{Sidelobe} in the case of uniform pdf can be found in [1].

[3]Note that in the case of uniform spatial distribution, the generalized hypergeometric function ${}_2F_3(\frac{1}{2}, \frac{3}{2}; 1, 2, 3; -(4\pi\tilde{R})^2)$ is used instead of ${}_1F_1(\frac{1}{2}; 1; -(4\pi\sigma)^2)$.

[4]Note that the corresponding characteristics in the case of uniform pdf can be found in [1].

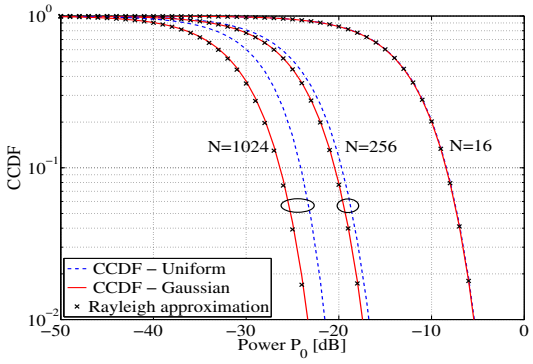

Fig. 5. CCDF for both uniform and Gaussian spatial distributions: $\phi = \frac{\pi}{4}$ and $\tilde{R} = 3\sigma = 2$.

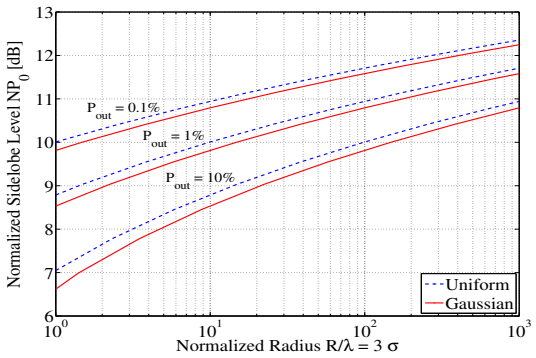

Fig. 6. The upper bounds on the sidelobe maximum with a given outage probability P_{out} for both uniform and Gaussian spatial distributions: N=16.

For large values of α, we can assume that $m_x = m_y = 0$ and $\sigma_x^2 = \sigma_y^2 = \frac{1}{2}$. Then, the CCDF follows a Rayleigh distribution and can be written as $\Pr[P(\phi) > P_0] = e^{-NP_0}$.

The CCDF for both uniform and Gaussian spatial distributions are shown in Fig. 5. It can be seen from the figure that for large values of N, the CCDF in the case of Gaussian pdf is lower than the CCDF in the case of uniform pdf. Therefore, the probability of exceeding a certain beampattern value P_0 is less in the case of Gaussian spatial distribution. Moreover, the aforementioned Rayleigh approximation remains valid in the case of Gaussian pdf, while it deviates from the actual CCDF in the case of uniform spatial distribution.

Another characteristic, which is used to describe the random behavior of sample beampattern, is the outage probability of sidelobes P_{out}. This characteristic can be used to estimate the maximum possible interference to other clusters in the neighborhood, and the probability of a given interference level to other clusters in the neighborhood. The upper bound on the outage probability P_{out} in the case of Gaussian spatial distribution can be found as

$$P_{\text{out}} \leq 8\sqrt{\pi}\sigma\sqrt{NP_0}e^{-NP_0}, \;\; NP_0 > \frac{1}{2}. \tag{14}$$

Fig. 6 illustrates the upper bounds on the sidelobe maximum with a given outage probability for both uniform[5] and Gaussian spatial distributions. It can be seen that for the same number of sensor nodes N and outage probability P_{out}, the level of interference to neighboring clusters is lower in the case of Gaussian spatial distribution and the value of the maximum peak in the sidelobe region increases with increasing the normalized radius $\tilde{R} = 3\sigma$.

5. CONCLUSIONS

A Gaussian pdf was proposed as a realistic model for spatial distribution of sensor nodes within a cluster of WSN. The average beampattern and its characteristics were derived. The distribution function of the beampattern level in the sidelobe region and the upper bound on the outage probability of the sidelobes were analyzed. It was shown that the collaborative beamforming for WSN provides better performance characteristics if sensor nodes are deployed according to a Gaussian pdf rather than a uniform pdf.

[5]Note that the upper bound on the outage probability in the case of uniform spatial distribution is given as [1]: $P_{\text{out}} \leq 4\sqrt{\pi}\tilde{R}\sqrt{NP_0}e^{-NP_0}$, $NP_0 > \frac{1}{2}$.

6. REFERENCES

[1] H. Ochiai, P. Mitran, H. V. Poor, and V. Tarokh, "Collaborative beamforming for distributed wireless ad hoc sensor networks," *IEEE Trans. Signal Processing*, vol. 53, no. 11, pp. 4110–4124, Nov. 2005.

[2] R. Mudumbai, G. Barriac, and U. Madhow, "On the feasibility of distributed beamforming in wireless networks," *IEEE Trans. Wireless Communications*, vol. 6, no. 5, pp. 1754–1763, May 2007.

[3] Y. Lo, "A mathematical theory of antenna arrays with randomly spaced elements," *IEEE Trans. Antennas and Propag.*, vol. 12, no. 3, pp. 257–268, May 1964.

[4] M. Donvito and S. Kassam, "Characterization of the random array peak sidelobe," *IEEE Trans. Antennas and Propag.*, vol. 27, no. 3, pp. 379–385, May 1979.

[5] M. Leoncini, G. Resta, and P. Santi, "Analysis of a wireless sensor dropping problem in wide-area environmental monitoring," *Proc. 4th Intl Symposium on Information Processing in Sensor Networks (IPSN 2005)* , Apr. 2005, pp. 239–245.

[6] M. Ahmed and S.A. Vorobyov, "Collaborative Beamforming for Wireless Sensor Networks with Gaussian Distributed Sensor Nodes," *Submitted to IEEE Trans. Wireless Communications.*